Available online at www.sciencedirect.com

ScienceDirect

Materials Today: Proceedings 5 (2018) 2049–2055

materialstoday: PROCEEDINGS

www.materialstoday.com/proceedings

ICMS 2017

Size control synthesis and amperometric sensing activity of Palladium nanoparticles for Glucose detection

A Mahajan, S Banik, S Roy Chowdhury, P. S.Roy and S. K.Bhattacharya*

Jadavpur University, Kolkata-700032, India

* Corresponding author. Tel.: +919831699643; fax: +913324146584.
E-mail address: skbhatt7@yahoo.co.in

Abstract

Size controlled synthesis of palladium nanoparticles of varying average diameter ranging from 8.1 to 21.3 nm, was executed by controlling the time of reflux of the facile reduction of $PdCl_2$ in a single pot using citric acid as reducing agent in presence of the steric stabilizer poly vinyl alcohol in water . The as synthesized nanomaterials were analysed by different microscopic techniques and utilized for the construction of a few anode-catalysts for biosensing of glucose. The catalytic activity of the anodes was characterized by cyclic voltammetry and chronoamperometry in different glucose solutions of varying concentration in 0.1M aqueous alkali. The maximum sensitivity is 66.2 μA cm^{-2} mM^{-1} found at the potential of 0.1V with respect to HgO/Hg electrode, for the particles having optimum crystallite-diameter of 12nm obtained from the solution having reflux time of 1.5 hour. The lowest limit (8.33 μM) and long linear range of detection (8.33 to 166 μM) are also important parameters of the best sensor studied. The results seem to help a better understanding and improvement of Palladium-based amperometric glucose sensor.

Selection and/or Peer-review under responsibility of Second International Conference on Materials Science (ICMS2017).

Keywords: Palladium nanoparticles, amperometric glucose biosensor

1. Introduction

In the last decade, nanoscience and technology have offered exciting prospects in biosensors by introducing novel nanomaterials, which include, but are not limited to, nanotubes, quantum dots, nanofibers, nanorods, and nano plates etc. [1, 2]. Possessing a number of remarkable advantages over conventional materials, nanomaterials are suitable for integration into novel mini, micro and nanodevices. These features use ultra-small sizes, large surface to volume

Selection and/or Peer-review under responsibility of Second International Conference on Materials Science (ICMS2017).

ratio, unique intermediate behaviour between bulk molecules and single one, high chemical reactivity, and electron confining property [3]. These special characteristics of nano-sized materials make them potential candidates in biotechnology and bio-analytical chemistry. Besides, nanoparticles have been extensively used in electro analysis due to their unique capabilities to enhance mass transport, facilitate catalysis, increase surface area, and control of micro environment of an electrode [4, 5]. Precious metal nanoparticles make excellent catalysts owing to their high ratio of surface atoms with free valences to the cluster of total atoms [6]. For example, platinum (Pt) and palladium (Pd) nanoparticles are especially effective to the redox reaction of hydrogen peroxide [7]. Further, metal nanoparticles could even provide electrochemical reversibility for redox reactions, which is not possible on the bulk metal electrode [8]. Thus metal nanoparticles (MNPs) have found numerous applications in many biomedical disciplines. Recently, MNPs have found extensive application in glucose biosensors by enhancing surface area and contributing to electron transfer from enzyme to electrode, which subsequently leads to improvement in detection of signal. Furthermore, the magnetic nature of MNPs facilitates the assembly of the GOx-bound NPs on the electrode surface [9]. Several palladium nanoparticles-based enzyme-free biosensors have also been reported in the literatures of detecting of glucose. These exhibit effectively improved sensitivity and selectivity towards the oxidation of glucose [10]. The first enzyme electrode and amperometric enzymatic biosensors were urbanized by Clark and Updike in the 1960s [11-13]. Since then the electrochemical glucose sensors based on glucose oxidase (GOx) have been widely investigated due to their high sensitivity, specificity and low detection limit [14-15]. Environmental conditions such as temperature, pH, humidity and the presence of ionic detergents in the sample can easily affect the performance of the GOx sensors [16]. As a result, there is an unmet necessity for a simple, stable, reliable and efficient sensor for direct non-enzymatic measurement of glucose levels in blood and other samples. Over the past decade the improvement of non-enzymatic glucose sensors has enlarged at an extensive rate. The expansion of an ideal glucose sensor must be an important concern for the biosensor industry. Numerous processes have been developed to create new glucose biosensors such as electrochemical methods [17], conductometry [18], colorimetry [19], optical methods [20] and fluorescent spectroscopy [21]. In the first generation glucose sensors, either the consumption of oxygen or formation of H_2O_2 is measured with respect to Standard Hydrogen Electrode (SHE). The sensor of second generation utilizes redox couple as a mediator to transfer the electron from solution phase to the electrode at a relatively lower potential. In the third generation sensors, biocatalyst sends the electrodes to the metal usually through a semiconductor like ZnO and acts at a much lower potential. In the fourth generation glucose sensor, glucose is directly oxidized on the metal surface leaving electrons on the metal. Since it is direct electron transfer, the current density generated and hence the sensitivity is expected to be the highest among all the different types of the sensors.

2. Experimental

2.1. Materials

Polyvinyl alcohol (PVA, average molecular weight = 125,000) acting as steric stabilizer, Palladium chloride ($PdCl_2$) with a purity of 99% and Citric acid from Merck, India were used in our experiment. Other reagents were at least AR/GR grade and used without further purification. Millipore (synergy) water was used throughout the reaction.

2.2. Synthesis of PVA coated Pd nanoparticles and preparation of glucose solution

PVA protected palladium nanoparticles for electrocatalysis of methanol oxidation were prepared by a previously developed method [22, 23].Here, ~1g PVA (0.008 mmol) and 50mL water were kept overnight for dissolving. 45 mL water, 0.864g citric acid (4.5 mmol) and 4 mL of 2 mass% $PdCl_2$ (0.45 mmol) in 2N HCl were added on the next day. Then reflux started in an O_2 free environment using $CaCl_2$-alkaline pyrogallol guard tube. The solutions were taken at a certain intervals of 0.33, 0.5, 1, 1.5 and 2 hour from the starting time of reflux to get colloidal palladium nanoparticles of different average diameters trapped into PVA matrix (Pd/PVA).

2.3. Preparation of electrodes

The mid portion of the rectangular strip of Ni-foil was wrapped with Teflon tape keeping both ends bare. The chemical deposition of palladium was executed on the two sides of the rectangular planar part of the foil and the other end was kept bare for electrical connection. Each of the Ni supported electrode was prepared by deposition of Pd solution using "dip and dry" method of chemical solution deposition. The process was applied to construct all the dip-coated electrodes designated as Ni/Pd(i) (i= 1-5) used in the electrochemical and SEM studies. For each electrode, the loading of Pd was computed from the mass and composition of the deposit.

2.4. Characterization of electrodes

The surface morphology of the prepared anodes was investigated with SEI INSPECT F 50 Field emission scanning Electron Microscope (FE-SEM). Surface composition of the anode catalyst was analyzed by energy dispersive X-ray (EDX) spectroscope coupled with the FE-SEM instrument. The shape and size of the particles were investigated by transmission electron microscope.

2.5. Electrochemical measurements

The electrochemical measurements were conducted in a two compartment glass-cell suitable for a conventional three-electrode assembly at 298.15K. The reference electrode in all electrochemical measurements was $Hg/HgO/OH^-$ (1M) (MMO) which had an equilibrium electrode potential ~ 0.10V with respect to the standard hydrogen electrode (SHE). In all the electrochemical measurements a large Pt-foil (1 cm × 1 cm) was used as counter electrode and potential data were recorded with respect to MMO. Cyclic Voltammetry and Chronoamperemetry were carried out using a computer aided Potentiostat/Galvanostat of AUTOLAB PG STAT 12 (Eco Chemic, Netherlands). Cyclic Voltammogram(CV) of each electrode immersed in 0.1M NaOH solution with and without glucose was recorded at the scan rate 50 mVs^{-1} for several consecutive cycles until steady CV was obtained.

3. Result and discussion

3.1. SEM and TEM study

In order to study the morphology of the as-synthesized Pd nanoparticles on the surface of Ni/Pd(i) (i=1-5) electrodes, scanning electron microscopic(SEM) study has been performed. The SEM image in Fig.1a and 1b show the overall morphology of the Ni/Pd (1) and Ni/Pd(4) electrode which are considered as representatives of all the Ni/Pd(i) (i=1-5) electrodes in low resolution. The pictures show some white spots which seem to be of nanoparticle PVA composites (Pd/PVA) which are supposed to adhere to one another or linked together via polymer. The polymer bedsare shown to be relatively smooth surface on which Pd nanoparticles are deposited. Although the particles are not well separated as in the TEM images as expected because of greater extent of catalyst loading on the electrode surface, the average diameter of the nanoparticles obtained from the SEM images are found to be 6.9, 8.1,.11, 12 and 21.3 nm respectively for the electrodes Ni/Pd (i) (i=1-5). It is worth mentioning that these values are in good agreement with those obtained from TEM and our previous study [22].

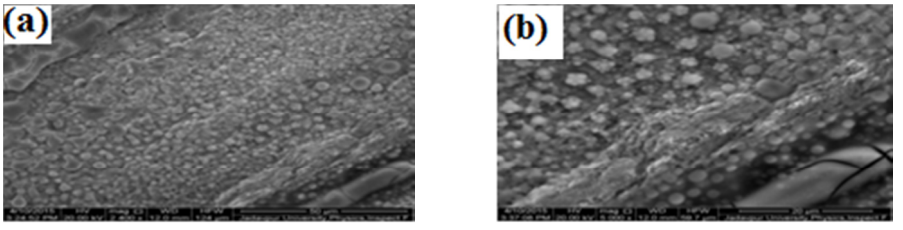

Fig 1.SEM images of (a) Ni/Pd(1) and (b) Ni/Pd(4)electrodes

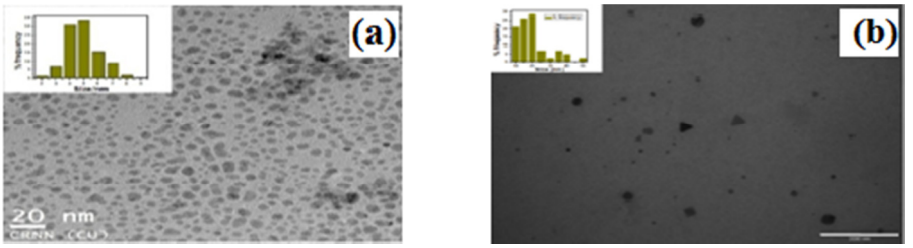

Fig 2.TEM image of Ni/Pd(1) and Ni/Pd(4) electrodes of average size about 6.3 nm and 12 nm respectively

Fig. 2a and 2b show the TEM images and corresponding size distribution bar diagrams of Pd nanoparticles (at the inset). It clearly appears from the TEM micrograph that the PVA-stabilised nanoparticles have different but mainly globular in shape and almost well separated as found in our previous study [23].The TEM study reveals that average diameter of the nanoparticles having reflux times are 0.33 and1.5 hour are 5.9 nm and 17 nm respectively. This indicates that the average size and polydisperse characteristics of the particles increase with time of reflux.

3.2. Cyclic voltammetry

The cyclic voltammograms (CVs) of bare Ni-foil (inset) and Ni/Pd(i) (i=1-5) electrodes immersed in the 133.9 μM glucose in 0.1M NaOH solution have been presented in Fig. 3(a).The cyclic voltammograms reveal that a pair of peaks due to hydrogen desorption in the potential range -0.8 to-0.5 and two peaks for formation of $Ni(OH)_2$ and PdO followed by formation of NiOOH in the subsequent potential range for the forward scan of potential [22]. The current densities of all these peaks are increased on addition of glucose indicating Pd mediated oxidation of glucose at various different potentials. For each profile the peak at 0.1V corresponds to PdOH formation:

$Pd+OH^- = PdOH+e^-$. (1)

The increase in current at the peak near 0.1V for different electrodes on addition of glucose indicates oxidation of glucose (I) to gluconate ion in presence of MOH (M= Ni, Pd) on the surface by the following reaction:

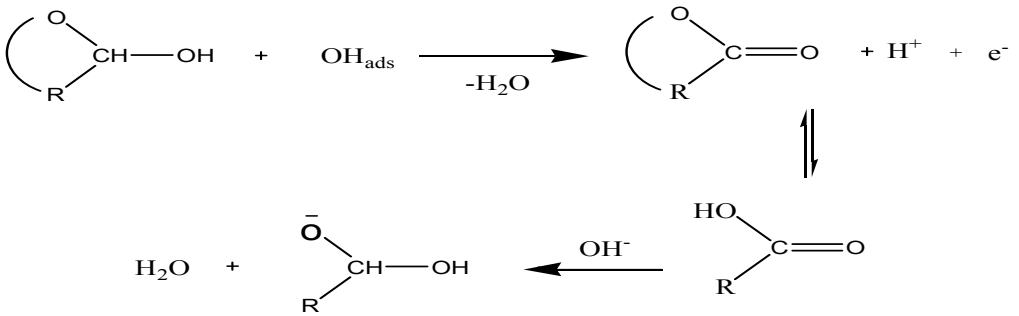

In the reverse scan of potential, first Ni(II) is converted to Ni(III) and then PdO to Pd as explained in our earlier study [22]. The peak currents at 0.1V follows the order: Ni/Pd(4)>Ni/Pd(2)>Ni/Pd(1)>Ni/Pd(3)>Ni/Pd(5), indicating that Ni/Pd(4) is the best electrode studied for glucose oxidation. The apparent anomalous behaviour as depicted in Fig.3a is explained by considering the fact that with increasing size, nanoparticle-PVA interaction will decrease and hence the capability of the reaction molecule to approach to the surface of the catalyst, will increase and so the reaction rate tend to increase with increase in size despite the decrease in surface area of the catalyst. Because of the two opposite trends of decreased surface area and increased available surface of the catalyst on increasing the diameter of the nanoparticles, the reaction rate passes through a maximum for an intermediate particle diameter. Being influenced by this two opposing effects the rate of reaction and hence sensitivity become maximum at an optimum radius of the synthesized Pd nanoparticles and this is found for electrode Ni/Pd(4).

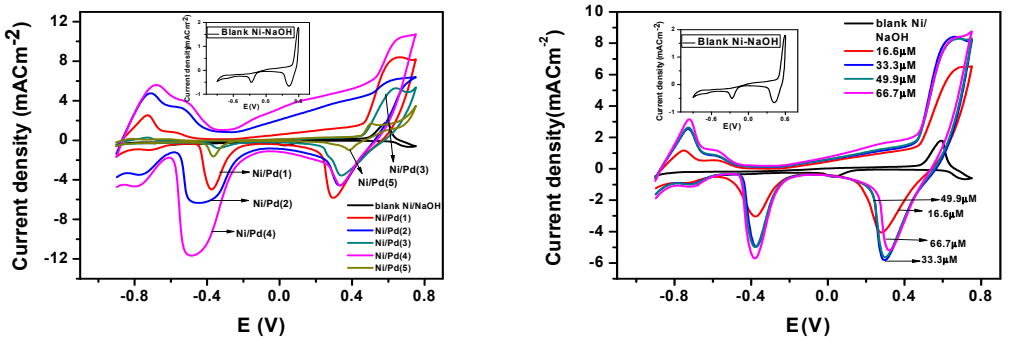

Fig 3 (a).CV of Ni/Pd(i) (i=1-5) electrodes at the concentration of 133.9 µM solution of glucose **(b)** CV of Ni/Pd(4) in absence and at different conc. of glucose

The Fig. 3b represents that cyclic voltammograms of Ni/Pd(4) in absence and presence of glucose of various concentrations. This shows that there is a significant eletrocatalytic response (i.e. glucose sensing) for the electrode Ni/Pd(4) as compared to bare Ni. Since with addition of glucose oxidation peak height is increased, the modified electrode is a potential candidate of glucose sensor

3.3. Chronoamperometry

Fig.4 represents that CA profiles of Ni/Pd(4) electrode at different glucose concentrations at constant potential of 0.1V. This shows that steady state current is increased with increasing the concentration of glucose. The oxidation occurs simultaneously with PdO phase generation and at lower concentration of glucose the latter dominates over glucose oxidation as evident from the reverse nature of the profile as compared to the usual one.

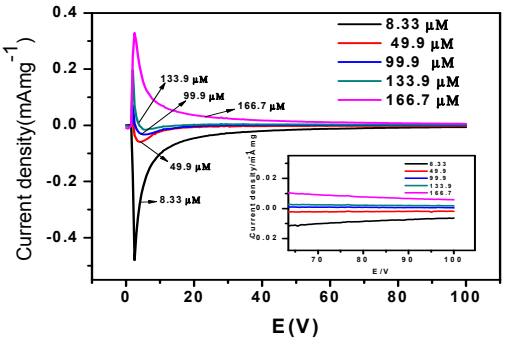

Fig. 4. Chronoamperometry profile of Ni/Pd(4) electrode at different concentration of glucose at 0.1V

The profiles showing the increase of the steady state current densities with concentration are presented in the inset of Fig. 4, which are the enlarged parts of different profiles in the steady state region.

3.4. Sensitivity and linear range

Chronoamperometric current–time response of Ni/Pd(4) electrode was measured at constant potential of 0.1V by successive addition of glucose (Fig. 5a). The calibration curve (Fig. 5b) for electrode Ni/Pd(4) exhibits a detection range from 8.33 µM to 166 µM with a sensitivity of 66.2 $\mu AmM^{-1}cm^{-2}$ and correlation co-efficient 0.987. This shows a very rapid and sensitive response of Ni/Pd(4) to the addition of glucose.

Table 1:Variation of different parameters of the anode-sensors with the diameter of the synthesized Pd nanoparticles

Name of the Electrode	Diameter of the synthesized Nanoparticles(nm)	Potential (V) vs Hg/HgO	Linear Range Of Concentration (μM)	Sensitivity ($\mu AmM^{-1} Cm^{-2}$)	Response time(s)
Ni/Pd(1)	6.9	0.1	0.833-19.9	12.5	5
Ni/Pd(2)	8.3	0.1	1.66-398	20.9	5
Ni/Pd(3)	11	0.1	8.33-66.7	53.5	5
Ni/Pd(4)	12	0.1	8.33-166	66.2	5
Ni/Pd(5)	21.3	0.1	1.66-333	19.8	5

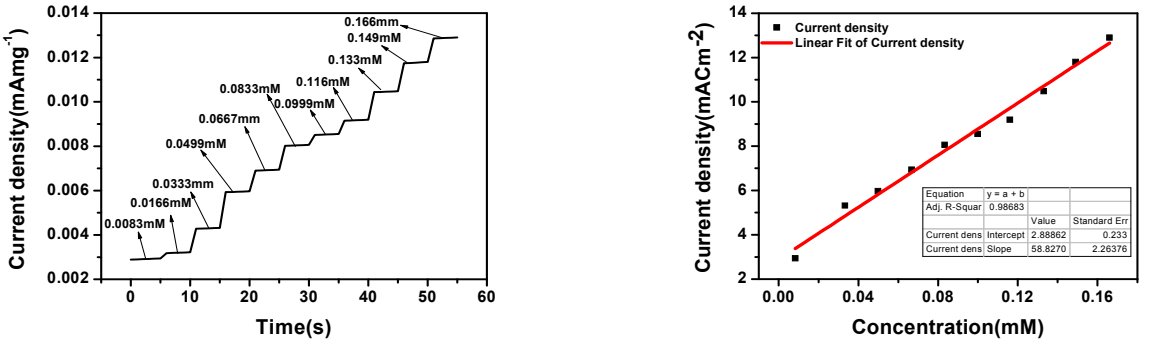

Fig 5 (a) Current–time response of Ni/Pd(4) electrode measured at 0.1V in succesive addition of glucose **(b).**Linear fit of Current density vs Concentration of Ni/Pd(4) electrode measured at 0.1V in successive addition of glucose

Linear fit of the data points in Fig. 5b for the representative electrode Ni/Pd(4) suggests that the electrode has very good glucose sensing activity when subjected to chronoamperometric oxidation. The sensitivity vs particle size plot in Fig. 6 depicts that sensitivity increases initially, reaches a maximum and then decreases with the diameter of the particles. The maximum corresponds to the particle diameter of size of 12 nm. The variation of different parameters of the anode sensors with the diameter of the synthesized Pd nanoparticles has been presented in Table 1.

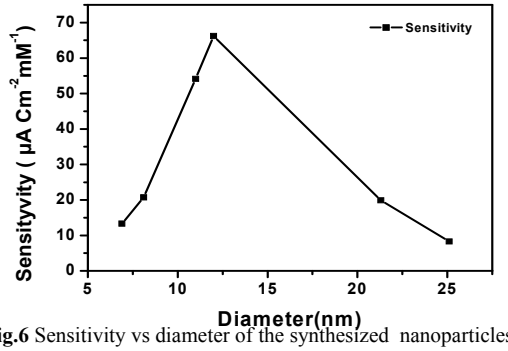

Fig.6 Sensitivity vs diameter of the synthesized nanoparticles

Increase of sensitivity with decrease in size reflects increased catalytic activity of the smaller nanoparticles. This activity is increased because of the increased effective surface area of the catalyst available to the approaching reactant molecules and the decreased activation energy of the reaction due to the presence of high energy surface molecules in the catalyst. On the other hand, the increase in catalytic activity with increase of particle diameter might be due to decreased PVA-particle interaction which overcomes the other factors.

4. Conclusion

- Several novel and cost effective non enzymatic glucose sensors based on Pd nanoparticles of various diameters are constructed.
- All the electrodes show high sensitivity, long-term stability and wide linear concentration range for sensing glucose.
- The highest sensitivity is obtained for electrode constructed with synthesized Pd nanoparticles of diameter 12nm.
- The sensitivity can be increased both by decreasing size of the nanoparticles and removing polymer environment from the nanoparticle surface.

Acknowledgement

The authors like to thank Jadavpur University and also Department of Science and Technology (INSPIRE Fellowship), New Delhi (IF140929) for financial support.

References

[1] A. A. Saei, P.N. Marandi, A.Abhari, M de la Guardia, J.E.N. Dolatabadi, Trends Anal. Chem. 42 (2013) 216-227.
[2] K. J. Cash, H.A. Clark, Trends Mol. Med. 16 (2010) 584-593.
[3] G. Cao, Nanostructures &Nanomaterials: Synthesis, Properties & Applications, Imperial College Press, London, UK, 2004.
[4] J Lu, I Do, L. T. Drzal, R. M. Worden, I Lee, ACS nano2 (9) (2008)1825–1832.
[5] C. W Welch, R. G Compton, Anal. Bioanal. Chem. 384 (2006) 601–619.
[6] S Hrapovic, E Majid, Y Liu; K Male; J. H Luong, Anal. Chem.78 (2006) 5504–5512.
[7] S. A. Miscoria, G. D. Barrera, G. A. Rivas, Electroanalysis14 (2002) 981–987.
[8] E Katz; I Willner,J Wang, Electroanalysis, 16 (2004) 19–44.
[9] J. Li, X. Wei, Y. Yuan, Sens. Actuators B 139 (2009) 400-406.
[10] L.M. Lu, H.B. Li, F Qu, X. B. Zhang, G. L. Shen, R. Q. Yu, Biosensors and Bioelectronics 26 (2011) 3500–3504.
[11] G Wang, X He, L Wang, A Gu, Y Huang, B Fang, B Geng, X Zhang, Microchim. Acta 180 (2013) 161-186.
[12] S.J. Updike, G.P. Hicks, Nature 214 (1967) 986–988.
[13] L.C. Clark, C Lyons, Ann N Y Acad Sci 102(1962) 29–45.
[14] T.W. Tsai, G Heckert , L.F. Neves, Y.Q. Tan, D.Y. Kao , R.G. Harrison, D.E. Resasco, D.W. Schmidtke, Anal Chem 81(2009) 7917–7925.
[15] N. K. Sarkar, S. K. Bhattacharya, Nanotechnology 24 (2013) 225502-225509.
[16] R Wilson, A.P.F. Turner, Biosens Bioelectron 7 (1992) 165–185.
[17] Y Wang, H Xu, J Zhang, G Li, Sensors 8 (2008) 2043–2081.
[18] Y Miwa, M Nishizawa, T Matsue, I Uchida, Bull Chem Soc Jp 67 (1994) 2864–2866.
[19] M Morikawa, N Kimizuka, M Yoshihara , T Endo,. Chem. Eur J 8 (2002) 5580–5584.
[20] S Mansouri , J. S. Schultz, Nat Biotech 2 (1984) 885–890.
[21] J.C. Pickup, F Hussain , N. D. Evans, O. J. Rolinski, D. J. S. Birch, Biosens Bioelectron 20 (2005) 2555–2565.
[22] P.S. Roy, J. Bagchi, S.K. Bhattacharya, Transition Met Chem, 34 (2009) 447-453.
[23] P.S. Roy, S. K. Bhattacharya, RSC Adv. 4 (2014) 13892-13900.